

Research article

Xinxin Jin, Guohua Hu, Meng Zhang*, Tom Albrow-Owen, Zheng Zheng and Tawfique Hasan

Environmentally stable black phosphorus saturable absorber for ultrafast laser

<https://doi.org/10.1515/nanoph-2019-0524>

Received December 16, 2019; revised December 25, 2019; accepted December 26, 2019

Abstract: Black phosphorus (BP) attracts huge interest in photonic and optoelectronic applications ranging from passive switch for ultrafast lasers to photodetectors. However, the instability of chemically unfunctionalized BP in ambient environment due to oxygen and moisture remains a critical barrier to its potential applications. Here, the parylene-C layer was used to protect inkjet-printed BP-saturable absorbers (BP-SA), and the efficacy of this passivation layer was demonstrated on the stable and continuous operation of inkjet-printed BP-SA in harsh environmental conditions. BP-SA was integrated in an erbium-doped ring laser cavity and immersed in water at $\sim 60^\circ\text{C}$ during operation for investigation. Mode-locked pulses at $\sim 1567.3\text{ nm}$ with $\sim 538\text{ fs}$ pulse width remained stable for $>200\text{ h}$. The standard deviation of spectral width, central wavelength, and pulse width were 0.0248 nm , 0.0387 nm , and 2.3 fs , respectively, in this period, underscoring the extreme stability of BP-SA against high temperature and humidity. This approach could enable the exploitation of BP-based devices for photonic applications when operating under adverse environmental conditions.

Keywords: 2D materials; black phosphorus; fiber laser.

1 Introduction

Ultrashort pulsed fiber lasers are an attractive light source for their flexibility, reliability, and compact integration [1], leading to a variety of applications such as industrial manufacturing, laser range finding, and materials processing. For generation of stable short pulses, saturable absorbers (SA) – nonlinear optical devices that provide loss modulation, absorbing lower-intensity light more strongly than higher-intensity light and thus promoting pulse generation – are widely deployed in fiber laser cavities, enabling mode-locking [2]. The key parameters of SAs are dynamic response (modulation depth and recovery time), operation wavelength range, and damage threshold. In addition, SA devices exhibiting stability under challenging operating conditions are of great importance for ultrafast lasers when deployed in practical applications [3].

Recent investigations on two-dimensional (2D) nanomaterials with versatile optical and electronic properties have facilitated new opportunities for photonic and optoelectronic applications, ranging from transistors and ultrafast photodetectors to SAs in ultrafast lasers. A number of 2D materials have been investigated and employed as SAs [e.g. graphene, semiconducting transition metal dichalcogenides (s-TMDs), and black phosphorus (BP)] to demonstrate reliable mode-locked performances in fiber lasers [4]. Among these, BP has emerged as a promising material with a direct bandgap varying from 0.3 eV in bulk to 2 eV in monolayer [5], bridging the gap between zero-gap graphene [6] and large-gap s-TMDs ($1\text{--}2\text{ eV}$). Like graphene, BP can be solution exfoliated to produce dispersions of high-quality single- and few-layer flakes when protected from oxygen and moisture [7]. Such dispersions can then be filtered to form films, blended with composites, or coated directly onto the substrates. They can also be exploited via printing techniques to allow for flexible, large-scale, high-speed, cost-effective fabrication [8] toward the commercial manufacturing of photonic devices. These flexible fabrication methods combined with wideband operation and ultrafast carrier dynamics have resulted in a variety of BP-based mode-locked lasers working from near- to mid-infrared regime [9–13].

*Corresponding author: Meng Zhang, School of Electronic and Information Engineering, Beihang University, Beijing 100191, China, e-mail: mengzhang10@buaa.edu.cn. <https://orcid.org/0000-0002-8217-042X>

Xinxin Jin: School of Electronic and Information Engineering, Beihang University, Beijing 100191, China

Guohua Hu: Cambridge Graphene Centre, University of Cambridge, Cambridge CB3 0FA, UK; and Department of Electronic Engineering, The Chinese University of Hong Kong, Hong Kong, China

Tom Albrow-Owen and Tawfique Hasan: Cambridge Graphene Centre, University of Cambridge, Cambridge CB3 0FA, UK

Zheng Zheng: School of Electronic and Information Engineering, Beihang University, Beijing 100191, China; and Beijing Advanced Innovation Center for Big Data-Based Precision Medicine, Beihang University, Beijing 100083, China

The prospects for the widespread practical applications of BP-based ultrashort pulsed lasers are still limited in part due to the unstable nature of BP in ambient conditions [14]. This could be further exacerbated in adverse environmental conditions during operation, such as high humidity and temperature [3]. The majority of the reported BP-based SAs without protection have thus shown extremely limited usable lifetime of 24 h [15]. Na et al. reported a passivation-stabilized BP-SA deposited on D-shaped fiber, enabling long-term pulse generation for >384 h in ambient environments [16]. It has been recently demonstrated that inkjet-printed and encapsulated BP-SAs may exhibit long-term (30 days) stability in modest ambient conditions [10]. However, stability against adverse operating conditions for similar devices, critical to their practical applications, are yet to be scrutinized. In this paper, it is shown that the stability of such protected BP-SAs can be significant by demonstrating highly stable, continuous mode-locking (>200 h) for stable pulse generation under complete water immersion at 60°C.

2 BP-SA fabrication and experimental setup

BP-SAs were fabricated on 1.5 μm polyethylene terephthalate substrate from inkjet printing of binary solvent-based inks of unfunctionalized BP flakes. This was followed by parylene-C protective layer deposition. Details on the ink formulation and characterization on BP degradation are available in Refs. [10, 11]. A set of SAs was fabricated without protective layer as control samples.

Before BP-SA was integrated into a fiber laser cavity, an open aperture Z-scan was used to investigate its intensity-dependent transmittance at 1.56 μm . The pump source was an ultrashort fiber laser, operating at 10 MHz repetition rate, and centered at 1562 nm with 150 fs pulse duration. BP-SA was swept through the focal plane of a beam from the laser source, and the transmitted power through SA was recorded as a function of incident light on the composite. Saturable absorption effect was confirmed by the increasing light transmittance as the pulse peak intensity increased. A typical dataset from a single measurement, at a fixed transverse position (Figure 1A), can be fitted using a two-level SA model, giving modulation depth $\alpha_0 = 12.57\%$, nonsaturation absorption $\alpha_{ns} = 9.98\%$, and saturation intensity $I_{sat} = 8.23 \text{ MW/cm}^2$.

The stability of BP-SA against high temperature and humidity was studied in an erbium-doped (Er-doped) fiber laser with anomalous dispersion. The experimental

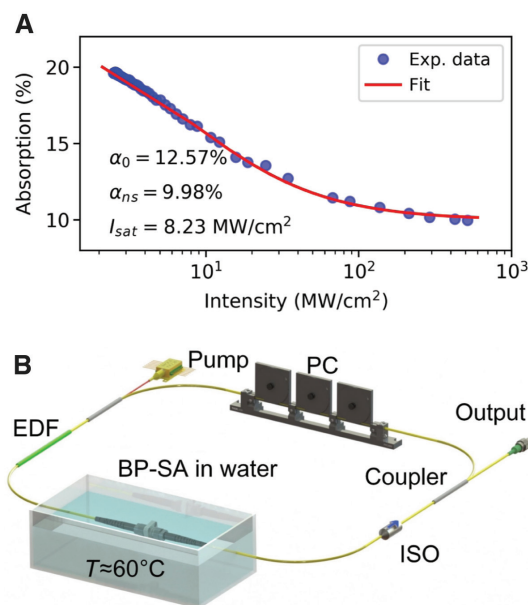


Figure 1: Nonlinear optical response of BP-SA and the schematic of the laser.

(A) Measured saturable absorption data and its corresponding fitting curve and (B) schematic of the fiber laser setup where BP-SA was immersed in water at $T \approx 60^\circ\text{C}$.

setup of the cavity is shown in Figure 1B, consisting of 0.7-m-long Er-doped fiber (EDF) with a group velocity dispersion of $-22.6 \text{ ps}^2/\text{km}$, copumped by 980 nm laser diode through a wavelength division multiplexer (WDM). An isolator (ISO) was used to ensure the unidirectional operation of the ring. A fiber polarization controller (PC) was inserted into the cavity for the optimization of cavity polarization state. The signal was delivered through a 10% fused-fiber coupler. The total cavity length for the cavity was 6.6 m and the net cavity dispersion β_2 was -0.13 ps^2 .

3 Results and discussion

To investigate the performance of BP samples under challenging operating conditions, a BP-SA without parylene-C protection was first integrated into the cavity by sandwiching between two fiber connectors and then completely immersed in water. The water was gradually heated up to $\sim 60^\circ\text{C}$ and kept at this temperature by a constant-temperature heat-up platform and was replenished every few hours to keep the level constant for the entire duration of the experiment. Self-start mode-locking with average output power of 0.3 mW was achieved at a pump power of 55 mW. Figure 2A–D shows the mode-locking performance of the unprotected BP-SA control sample-based fiber laser. The

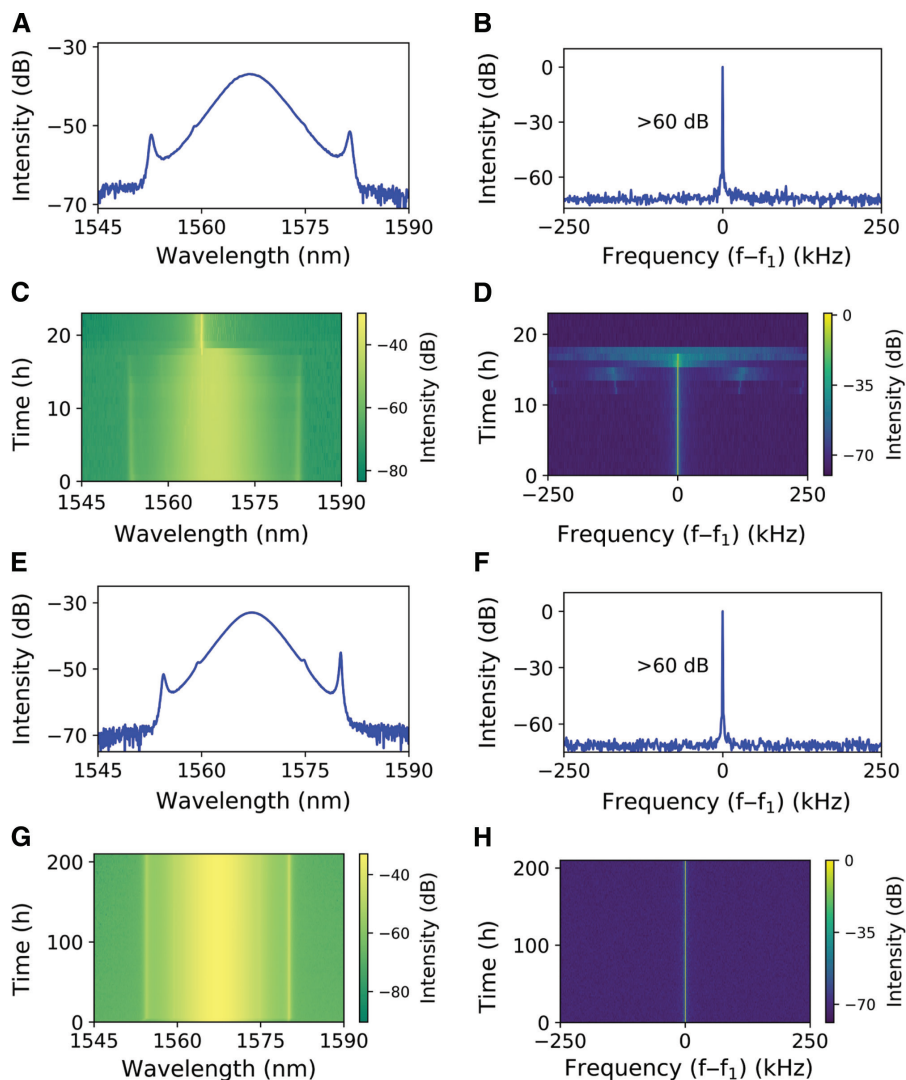


Figure 2: Mode-locking performance of the BP-SA.

Mode-locked (A) spectrum and (B) RF spectrum from unprotected BP-SA laser under water immersion, output (C) optical spectra and (D) RF spectra across 23 h from unprotected BP-SA laser under water immersion, mode-locked (E) spectrum and (F) RF spectrum from parylene-C-encapsulated BP-SA laser under water immersion, and output (G) optical spectra and (H) RF spectra across 200 h from parylene-C-encapsulated BP-SA laser under water immersion. $f_1 = 30.3$ MHz.

spectrum centered at 1566.9 nm had a full-width at half-maximum (FWHM) of 5.6 nm (Figure 2A). Figure 2B shows the radiofrequency (RF) spectrum on a span of 500 kHz, with a signal-to-noise ratio of >60 dB. Both optical and RF spectra were recorded every 1 h, showing the change in the mode-locking performance and degradation of the sample. As shown in Figure 2C and D, the laser first evolved into a continuous wave (CW) breakthrough after 13 h and then CW operation after 18 h. This is attributed to the water-induced degradation of the printed, unprotected BP [17].

The experiment was then repeated with the protected BP-SA sample under the same experimental condition. Self-start mode-locking with an average output power of

0.33 mW was achieved at the pump power of 55 mW. The optical spectrum shown in Figure 2E has a center wavelength of 1567.2 nm and FWHM bandwidth of 5.35 nm, and the RF spectrum shown in Figure 2F has a signal-to-noise ratio of >60 dB. Even under these extreme conditions, the protected BP-SA mode-locked laser showed stable continuous mode-locking for >200 h (Figure 2G and H).

The variation of spectral width and central wavelength vs. time in both cases was calculated further (Figure 3A). Before the unprotected BP-SA laser lost the mode-locked state at 18 h, although the central wavelength did not significantly change, the FWHM bandwidth decreased dramatically with sample degradation. In contrast, for the case of protected BP-SA laser, the spectral width and central

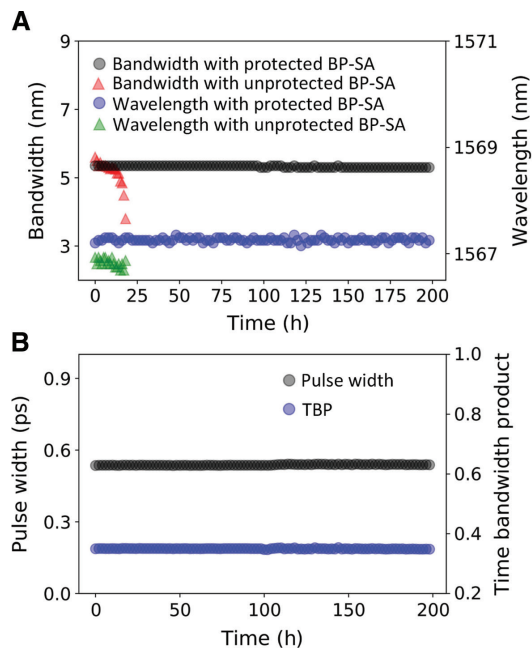


Figure 3: Long-term stability of the BP-SA.

Variations of (A) bandwidth and central wavelength under water immersion and (B) pulse width and TBP under water immersion from parylene-C-encapsulated BP-SA laser.

wavelength remained very stable. The average FWHM bandwidth and central wavelength were 5.33 and 1567.26 nm, respectively, during the 200 h measurement period. The standard deviation (SD) of spectral width and central wavelength were 0.0248 and 0.0387 nm, respectively, indicating no evident variation of intensity and spectral wavelength position. The pulse width and time bandwidth product (TBP) of the protected BP-SA were also calculated (Figure 3B). TBP was calculated as $\Delta\tau\Delta\lambda c/\lambda^2$, where $\Delta\tau$ is the pulse width, $\Delta\lambda$ is the FWHM bandwidth, λ is the center wavelength, and c is the light speed. The average pulse width was 537.9 fs, where a sech^2 temporal profile was assumed, with SD of 2.3 fs. The average TBP was calculated as 0.350, close to the Fourier transform limit of a sech^2 pulse, with SD of 0.001. It was noted that the device can potentially operate for much longer as the parameters of the laser remained unchanged when the measurement was terminated. These results demonstrated that parylene-C-encapsulated BP-SA indeed contributes to stable mode-locking operation under these adverse environmental conditions.

4 Conclusions

In summary, parylene-C passivation layers could enable unfunctionalized BP-SAs to stably work in adverse

operating conditions at $\sim 60^\circ\text{C}$ under complete water immersion for >200 h. The results contribute to a growing body of work focused on studying the long-term environmental stability of this novel direct bandgap material for photonic applications. This approach could also be adopted for other nanomaterial-based SAs whose performance varies over time due to subtle changes in operating conditions in real-life scenarios.

Acknowledgments: This work was supported by the National Natural Science Foundation of China (grants 51778030 and 51978024, Funder Id: <http://dx.doi.org/10.13039/501100001809>) and EPSRC (grant EP/L016087/1, Funder Id: <http://dx.doi.org/10.13039/501100000266>).

References

- [1] Zhang M, Kelleher EJR, Popov SV, Taylor JR. Ultrafast fibre laser sources: examples of recent developments. *Opt Fiber Technol* 2014;20:666–77.
- [2] Keller U. Recent developments in compact ultrafast lasers. *Nature* 2003;424:831–8.
- [3] Torrisi F, Popa D, Milana S, et al. Stable, surfactant-free graphene-styrene methylmethacrylate composite for ultrafast lasers. *Adv Opt Mater* 2016;4:1088–97.
- [4] Sun ZP, Martinez A, Wang F. Optical modulators with 2D layered materials. *Nat Photonics* 2016;10:227–38.
- [5] Xia F, Wang H, Jia Y. Rediscovering black phosphorus as an anisotropic layered material for optoelectronics and electronics. *Nat Commun* 2014;5:4458.
- [6] Novoselov KS, Fal'ko VI, Colombo L, et al. A roadmap for graphene. *Nature* 2012;490:192–200.
- [7] Kang J, Wells SA, Wood JD, et al. Stable aqueous dispersions of optically and electronically active phosphorene. *Proc Natl Acad Sci U S A* 2016;113:11688–93.
- [8] Hu GH, Kang J, Ng LWT, et al. Functional inks and printing of two-dimensional materials. *Chem Soc Rev* 2018;47:3265–300.
- [9] Zhang M, Wu Q, Zhang F, et al. 2D black phosphorus saturable absorbers for ultrafast photonics. *Adv Opt Mater* 2019;7:18.
- [10] Hu G, Albrow-Owen T, Jin X, et al. Black phosphorus ink formulation for inkjet printing of optoelectronics and photonics. *Nat Commun* 2017;8:278.
- [11] Jin XX, Hu GH, Zhang M, et al. 102 fs pulse generation from a long-term stable, inkjet-printed black phosphorus-mode-locked fiber laser. *Opt Express* 2018;26:12506–13.
- [12] Du J, Zhang M, Guo Z, et al. Phosphorene quantum dot saturable absorbers for ultrafast fiber lasers. *Sci Rep* 2017;7:42357.
- [13] Woodward RI, Majewski MR, Macadam N, et al. Q-switched Dy:ZBLAN fiber lasers beyond $3\ \mu\text{m}$: comparison of pulse generation using acousto-optic modulation and inkjet-printed black phosphorus. *Opt Express* 2019;27:15032–45.

- [14] Favron A, Gaufres E, Fossard F, et al. Photooxidation and quantum confinement effects in exfoliated black phosphorus. *Nat Mater* 2015;14:826–32.
- [15] Chen Y, Chen SQ, Liu J, Gao YX, Zhang WJ. Sub-300 femtosecond soliton tunable fiber laser with all-anomalous dispersion passively mode locked by black phosphorus. *Opt Express* 2016;24:13316–24.
- [16] Na D, Park K, Park KH, Song YW. Passivation of black phosphorus saturable absorbers for reliable pulse formation of fiber lasers. *Nanotechnology* 2017;28:475207.
- [17] Island JO, Steele GA, van der Zant HSJ, Castellanos-Gomez A. Environmental instability of few-layer black phosphorus. *2D Mater* 2015;2:6.